ISSN 0511-5728
The West Indian Journal of Engineering
Vol.43, No.1, July 2020, pp.26-35

Adsorption of Pb(II) and Phenol from Wastewater Using Silver Nitrate Modified Activated Carbon from Groundnut (*Arachis hypogaea L.*) Shells

Omodele A. A. Eletta [a], Ibrahim O. Tijani [b], and Joshua O. Ighalo [c,Ψ]

Department of Chemical Engineering, Faculty of Engineering and Technology, University of Ilorin, Ilorin, P. M. B. 1515, Nigeria.
[a]Email: modeletta@unilorin.edu.ng
[b]Email: ibrahimolaniyi21@gmail.com
[c]Email: oshea.ighalo@yahoo.com

[Ψ] *Corresponding Author*

(Received 17 February 2020; Revised 06 July 2020; Accepted 20 July 2020`)

Abstract: *This study was to remove Pb(II) and phenol from pharmaceutical wastewater using activated carbon derived from Silver nitrate modified groundnut (Arachis hypogaea L.) shells. The adsorbents were characterised by Fourier transform infrared spectroscopy (FTIR), scanning electron microscope (SEM) and X-ray Diffraction (XRD) analysis. The levels of Pb(II) and phenol in the effluent evaluated were 0.2 ppm and 3.7 ppm which were above the WHO standard. The optimal factors for Pb(II) and phenol removal by modified ground-nut shell activated carbon (MGSAC) were 176 minutes, 1.0 g/L adsorbent dosage, 35^{o}C and pH of 6.5. The numerical optimisation revealed that the optimal removal efficiency for Pb(II) and phenol adsorption are 99.6% and 99.4% respectively for MGSAC. The adsorption of both Pb(II) and phenol was best fit to Langmuir isotherm and pseudo-second order kinetic models. The monolayer adsorption capacity of the modified adsorbent for Pb(II) and phenol were 123.2 mg/g and 115.5 mg/g respectively. The adsorption process for both Pb(II) and phenol was exothermic and spontaneous.*

Keywords: *Adsorption, Activated carbon, Groundnut shell, Lead, Phenol, Environment*

1. Introduction

Pharmaceutical industry wastewater has been shown to contain a plethora of pollutants including lead and phenol (Araujo et al., 2018; Olarinmoye et al., 2016; Snyder et al., 2010). In a bid to achieve environmental sustainability, much research effort has been invested in the mitigation of these pollutants from the ecosystem (Adeniyi and Ighalo, 2019; Rani and Sud, 2015). Lead is a very toxic element, even at low concentrations. It affects the central nervous system, kidneys, liver, and gastrointestinal system, and it may directly or indirectly cause diseases such as anaemia, encephalopathy, hepatitis, and the nephritic syndrome (Wang et al., 2010). According to the USEPA, the permissible level for lead in drinking water is 0.05 mg/l (Sarkar et al., 2003).

Phenol is an organic pollutant that has potential toxicity to human health. Phenol can be found in wastewater from different chemical industries including pulp and paper, petroleum refinery, dye synthesis, coal gasification and pharmaceutical industries. Therefore, effective removal of phenol from the wastewater and reducing its concentrations to the permitted levels before discharging are challenging issues. The US Environmental Protection Agency (USEPA) regulations suggest phenol concentration below 1 ppm for wastewater (Abussaud et al., 2015). Adsorption is one of the most attractive approaches for heavy metals and phenolic compounds removal due to its high efficiency, simple and safe treating processes, versatility for different water systems and low cost.

Many adsorbents, including active carbons, chitosan, resins, and carbon nanotubes have been used for removal of heavy metals or/and phenolic compounds (Ighalo and Adeniyi, 2020a; Ighalo and Adeniyi, 2020c). However, there are some defects, such as low efficiency, bad stability and difficult separation, limiting their practical application (Yang et al., 2015). The mitigation of lead has been investigated in recent times using *Terminalia catappa* seed husk biochar (Canlas et al., 2019), live and dead cell mass of *Pseudomonas aeruginosa* (Ighalo and Adeniyi 2020d; Karimpour et al. 2018), organic acid modified rubber leaf powder (Fadzil et al., 2016), Sago bark (*Metroxylon sago*) powder (Fauzia et al. 2018), cacao pod (*Theobroma cacao*) rind waste (Eletta et al., 2020; Moelyaningrum, 2018), fish scales (Eletta and Ighalo, 2019; Ighalo and Eletta, 2020) and a host of others (Eletta et al., 2019). The mitigation of phenol has been investigated in recent times using steam activated biomass soot and tire carbon black (Trubetskaya et al., 2019), activated carbon from black wattle bark waste (Lütke et al., 2019), spent black tea leaves (Ali et al., 2018) and a host of others. There are no studies reporting groundnut shell used in this domain.

Groundnut (*Arachis hypogaea L.*) is one of the world's most popular oilseed crops which is grown as an

annual plant, but perennial growth is possible in climates which are warm until harvest. Its high content of oil and protein makes it an important commodity for both human use and livestock feed (Farag and Zahran, 2014). Groundnut shell is of low ash content, low apparent density, and a high degree of porosity which is assured as a good precursor to synthesis activated carbon (Babarinde and Onyiaocha, 2016). Thus, the conversion processing of groundnut shell for activated carbon could ease and reduce the environmental pollution of groundnut shell while making readily available, activated carbon at a reduced cost.

In this study, pharmaceutical wastewater was characterised to determine the level of pollutants present and what chemical species constitute an environmental problem in Ilorin, Nigeria. Phosphoric acid was used to produce activated carbon from groundnut shell at 500˚C and the activated carbon produced was further modified with silver nitrate. After comprehensive characterisation of its physiochemical properties, both adsorbents were applied to remove Pb(II) and phenol from wastewater respectively. The effect of contact time, dosage and temperature on the adsorption of Pb(II) and phenol from wastewater were determined. The adsorption isotherms, kinetics and thermodynamics were also investigated to analyse the adsorption mechanisms.

2. Methodology

2.1 Materials and Equipment

The reagents used for this study include: phosphoric acid (H_3PO_4), silver nitrate ($AgNO_3$), distilled water, phenol (C_6H_5OH), lead nitrate $Pb(NO_3)_2$ and all the chemicals used in this research were of analytical grade. The instruments used are, magnetic stirrer, ball mill, Scanning Electron Microscope (SEM) (Phenom prox, Netherlands), X-ray diffractometer (Bruker D2, Germany), Fourier Transform Infrared spectrophotometer (FTIR) (Nicoletin 10 MX), Branueur-Emmet-Teller analysis (BET) (Quantachrome FS240 NOVA 4200e), Muffle furnace (Sheffield LF4), EDX (JSM-6510LV, England), pH meter, Atomic Absorption Spectrophotometer (AAS) (GBC-902, Australia) and UV spectrophotometer (Model AA-680), respectively.

2.2 Analysis of Wastewater and Preparation of Simulated Water

The wastewater was sourced and analysed to establish pollutant(s) of interest before the synthesis of wastewater in the laboratory. The wastewater was sourced from a pharmaceutical company located at 8º 28’ N, 4º 33’ E in Ilorin, Nigeria. Five (5) litres of the liquid were collected.

The wastewater from the pharmaceutical industry was analysed using Atomic Absorption spectrophotometer (AAS) and UV spectrophotometer to determine the concentration of Pb(II) and phenol, respectively. For the stock solutions of simulated water, 1000 mg/L of Pb(II) and phenol was prepared by dissolving 1.6 g of lead nitrate and 1.0 g of phenol in 1000 mL deionised water. The stock solution was diluted with deionised water to the desired Pb(II) and phenol concentrations. After adsorption, the supernatant liquids were filtered with Whatmann filter paper.

2.3 Preparation of Adsorbents

Groundnut (*Arachis hypogaea L.*) shell was obtained from a local market and cleaned, sun-dried and further oven-dried at 80^0C until a constant weight is observed. Thereafter, size reduction was carried out using a ball mill followed by sieving and storage in a desiccator. 50 g each of the precursor was weighed into different beakers and the phosphoric acid solution was added to the precursor in 250 ml beakers based on the impregnation ratio of 1:2. The mixture was stirred continuously using a magnetic stirrer at room temperature for 5 hours thereafter, the mixture was stored for 24 hours (Yakout and El-Deen, 2016). The mixture was filtered and dried in an oven at 110˚C for 24 hours. The dried sample was carbonized directly in a furnace at 500 ˚C in an inert environment.

The activated carbon produced was screened to 100 µm micrometres and washed with 0.5 M phosphoric acid followed by distilled water at room temperature until the washing solution becomes neutral at pH 7. The activated carbon produced was dried in an oven at 110˚C for 6 hours and cooled to room temperature to obtain the H_3PO_4 activated carbon. Following the procedure described by Amuda et al. (2007), the activated carbon was modified by soaking in a freshly prepared silver nitrate solution (0.5 mg/l). 10 ml of the silver nitrate solution was mixed with 0.5 g of activated carbon in a conical flask, which is according to the method used by Olajire et al. (2016). Thorough mixing was carried out using a magnetic stirrer at 200 rpm to ensure thorough mixing. After the deposition of $AgNO_3$ onto the activated carbon, the silver nitrate modified activated carbon was filtered and dried in an oven at 110°C till dryness was observed. The adsorbent is referred to as modified ground-nut shell activated carbon (MGSAC) whilst the unmodified version was referred to as GSAC. The modification by silver nitrate was done to improve the surface functional groups, increase in adsorbate affinity for the adsorbent and impact a secondary anti-microbial property on the adsorbent.

2.4 Characterisation of the Activated Carbon

The groundnut shell activated carbon and silver nitrate modified activated carbon was characterised using FTIR (Nicoletin 10MX) to determine the functional groups responsible for the adsorption. The surface area was determined using Branueur-Emmett-Teller (BET) (Quantachrome FS240 NOVA 4200e) (Adeniyi et al., 2020), the elemental characteristics were obtained by EDX (JSM-6510LV, England).

2.5 Batch Adsorption Experiment

Batch adsorption studies were carried out on both the GSAC and MGSAC to evaluate their adsorption performances. The adsorption was performed by adding 0.1 g of activated carbon into 100 ml of synthesised wastewater in 250 ml conical flask, covered and agitated at 200 rpm using a mechanical shaker for 180 mins to ensure equilibrium at room temperature and pH 7.0 (Amuda et al., 2007). After this, the content was centrifuged at 500 rpm for 20 mins. The resulting solution was decanted into brownish bottles and stored for analysis. Whatman filter paper was used to filter the content and it was analysed using UV-Spectrophotometer for the residual concentration at 270 nm wavelength for phenol and Atomic Absorption Spectrophotometer for Pb (II). The adsorption capacity, (q_e) (mg/g) was evaluated by using Equation (1).

$$(q_e)\ (mg/g) = [(C_o - C_e)/v\ ] / M \quad (1)$$

Where C_o (mg/L) is the initial concentration of Pb(II) and phenol in contact with adsorbent, C_e (mg/g) is the final concentration of Pb(II) and phenol after the batch adsorption procedure at time t, m (g) is the mass of adsorbent and V is the volume of the adsorbate in litres (L). The percentage of removal was evaluated using Equation (2)

$$\text{Removal (\%)} = (C_o \text{ and } C_e) / C_o \quad (2)$$

Where C_o and C_e are the Pb(II) and Phenol concentration at initial state and equilibrium respectively.

2.6 Parametric Studies

The effect of contact time on adsorption was studied by setting up nine conical flasks on a mechanical shaker having 0.1 g of MGSAC separately, and GSAC in 100 ml of Pb(II) and phenol solutions of 25 mg/l, 50 mg/L, 75 mg/l, 100 mg/l, and 125 mg/l respectively, and agitated at 200 rpm at room temperature. The beakers were removed after contact times ranging from 10 to 180 minutes. The effect of adsorbent dose on the adsorption of Pb(II) and phenol was studied by varying the activated carbon dose between 0.2-1.0 g in nine conical flasks having 100 ml of 100 mg/l concentration of Pb(II) and phenol respectively (Gupta and Rafe, 2013). Each was then agitated at 200 rpm for 3 hours at room temperature. The effect of temperature was studied at intervals of 35˚C, 45˚C, and 55˚C.

3. Results and Discussion

3.1 Characterisation of Pharmaceutical Effluent

The produced wastewater from the pharmaceutical industry was analysed using AAS and UV spectrophotometer to measure the concentration of Pb(II) and phenol respectively. The results gotten show that the concentration of Pb(II) and phenol are 0.2 ppm and 3.7 ppm respectively which are above the maximum permissible limits by WHO (see Table 1). The maximum permissible limits of lead in different categories of water as proposed by different organisations standard are shown in Table 1. Phenol and phenolic compounds have been listed by several regulatory bodies on the priority pollutants list and have proposed the maximum permissible limits of phenol in different categories of water (see Table 2) (Sonawane and Korake, 2016).

Table 1. Maximum Permissible limit of Lead in Water

Standard	Type	Amount (mg/L)
WHO	Drinking water	0.01
USEPA	Wastewater	0.05

Table 2. Maximum Permissible limit of Phenol in Water

Agency	Type of water	Maximum permissible limit
USEPA	Wastewater	1.00 ppm
WHO	Drinking water	0.1 ppm

3.2 FTIR Spectra for the Adsorbent

The presence of various functional groups on the surface of the adsorbent was analysed with Thermo-Fisher FT-IR analyser (Scientific, Nicolet 5700) within the spectrum range of 400–4000 cm^{-1}. The presence of these functional groups on the activated carbon was responsible for adsorption of different heavy metal from aqueous solution (Rai et al., 2015). The FTIR of the GSAC and the MGSAC are shown in Table 3.

Table 3. The FTIR of the GSAC and the MGSAC and BET Analysis

Sample	Specific surface area (m^2/g)	Microspore volume (m^3/g)	Pore diameter (nm)	Pore width (nm)
GSAC	533.943	0.475	3.00	6.503
MGSAC	213.949	0.190	2.00	2.647

The IR peak observed in the MGSAC and GSAC ranged from 58.89-3772.1 cm^{-1} and 23.706 cm^{-1} and 3857.8 cm^{-1} respectively. The peak height ranged from 38.2-39.8 cm^{-1} and 14.3-17.8 cm^{-1} for both MGSAC and GSAC respectively. Changes were observed in the functional groups of both adsorbents. There was the appearance of the -C≡C- at peak of 2191.4 cm^{-1} after the modification of activated carbon. The images of both MGSAC and GSAC are shown in Figures 1 and 2, respectively.

The FTIR showed appearance, disappearance or broadening of the peaks after the carbonisation and impregnation with both phosphoric acid and silver nitrate (Olajire et al., 2016). There were changes in the functional groups of both samples and upon surface modification, there are appearances of some additional peaks at MGSAC that can be attributed to stretching vibration of OH.

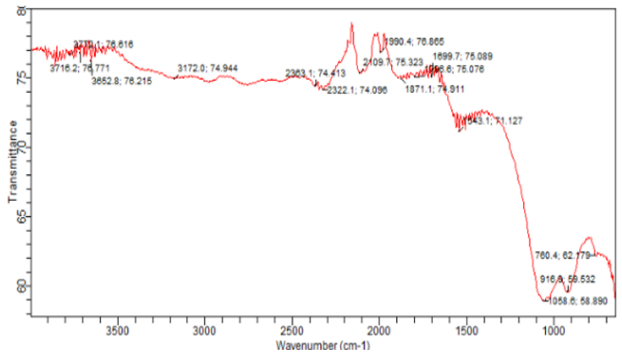

Figure 1. Modified groundnut shell activated carbon (MGSAC)

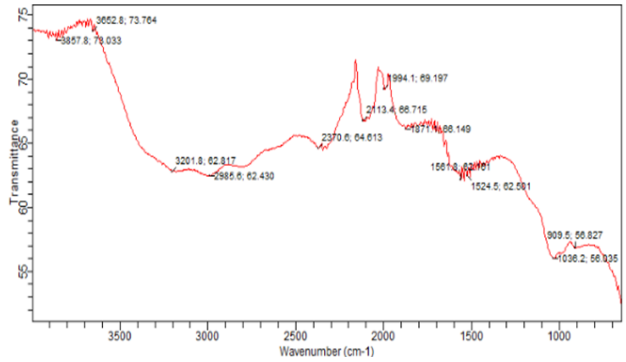

Figure 2. Groundnut shell activated carbon (GSAC)

3.3 Branueur-Emmet-Teller (BET) Analysis for the Adsorbent

The surface area was determined using Branueur-Emmett-Teller (BET) (Quantachrome FS240 NOVA 4200e). The results of the BET of both GSAC and MGSAC are shown in Table 3. The porosity of MGSAC was well developed albeit with lower surface area, microspore volume, and larger average pore diameter. The pore diameter of 3 nm and 2 nm for GSAC and MGSAC shows that the adsorbents are mesoporous. The range for mesoporous adsorbents is between 2 and 50 nm. The BET results also show that the unmodified adsorbent has a higher surface area than the modified one. The modification reduced the surface areas by over two times. This is because some of the pores of the adsorbent are occupied by the silver nitrate. However, another performance advantage is gotten from the utilisation of silver nitrate such as modification of surface functional groups, an increase in adsorbate affinity and the presence of a secondary anti-microbial ability of the adsorbent.

3.4 SEM-EDX for the Adsorbent

Figure 3 is the SEM image of GSAC and Figure 4 is the SEM image of MGSAC. These images were used to verify the possible changes in morphological features of the samples before and after the modification. As shown in Figure 3, the surface of the GSAC is irregular and relatively rough with a dense fibrous structure. This suggests the possibility of a high surface area for adsorption (Ighalo and Adeniyi, 2020b). After the modification with silver nitrate, Figure 4 shows that the surface of the MGSAC was regular and has more complex pore structures compared to the GSAC. These results indicated that the physical characteristics of GSAC that was modified with silver nitrate were improved. Also, it improved the accessibility of active sites and the adsorption of Pb(II) and phenol during the adsorption process. From the EDX analysis of the MGSAC (see Table 4), it was observed that the analysis of the EDX revealed the presence of C, O, Si, and P. The higher peak of carbon (C) in Table 4 was attributed to the effect of carbonisation of the groundnut shell at high temperature.

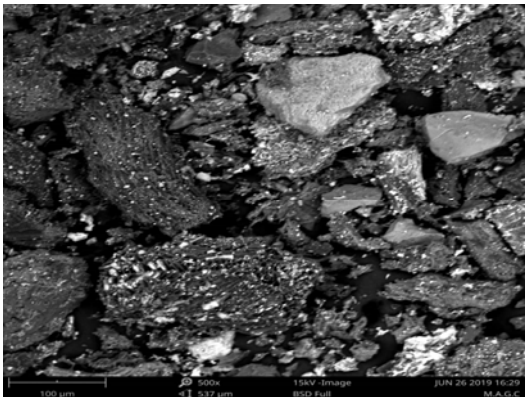

Figure 3. Groundnut Shell Activated Carbon (GSAC)

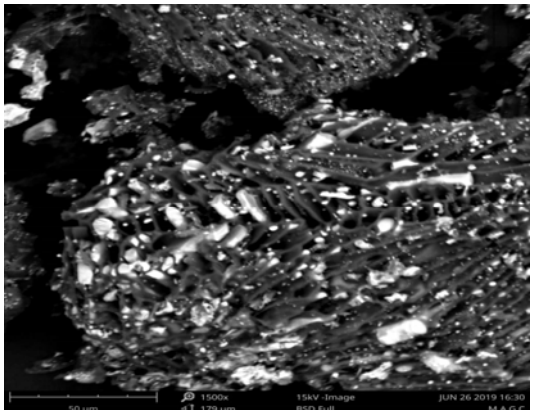

Figure 4. Modified Groundnut Shell Activated Carbon (MGSAC)

Table 4. Composition of the Elements in MGSAC

Element Number	Element Symbol	Element name	Atomic Conc.	Weight Conc.
6	C	Carbon	74.80	66.64
8	O	Oxygen	18.59	22.09
15	P	Phosphorus	2.15	4.94
14	Si	Silicon	1.23	2.56
7	N	Nitrogen	2.34	2.43
9	F	Fluorine	0.79	1.11
16	S	Sulfur	0.07	0.16
17	Cl	Chlorine	0.04	0.11

3.5 Parametric Studies

3.5.1 Effect of Contact Time

The effect of contact time on adsorption of Pb(II) and phenol onto prepared GSAC and MGSAC are shown in Figures 5-8. These were conducted at 25 mg/L initial concentration, 25˚C, 200 rpm shaking speed and 0.2 g adsorbent in 100 ml aqueous solution. The result revealed that the uptake of adsorbate increased at the initial stage of the contact time for all the concentrations (Ighalo et al., 2020a; Mall et al., 2006). This is because, at the beginning of the adsorption process, all the active sites on the adsorbent are vacant. Hence, adsorption proceeds at a faster rate and desorption at a lower rate as the active sites get occupied (Ighalo et al., 2020b; Rashid et al., 2016). For an initial concentration of 25 mg/L, the adsorption capacity and percentage removal of the MGSAC were higher compared to the GSAC as shown in Figures 6-9. This is the same for all other domain of initial concentrations. It was also discovered that the percentage removal of Pb(II) and phenol also increased with increasing time. This is because more pollutant molecules move through the solid-liquid film with time onto the adsorption sites. At equilibrium virtually, all pores are filled hence there is no significant uptake of the pollutant species anymore.

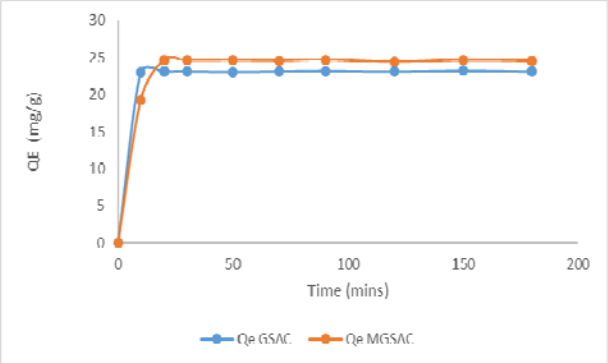

Figure 5. Effect of Contact Time on Adsorption of Pb(II) (at 25 mg/L initial concentration)

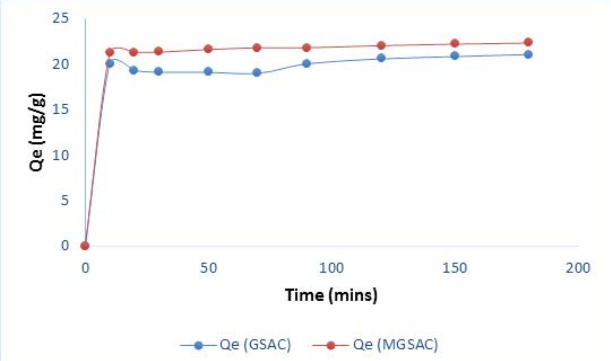

Figure 6. Effect of Contact Time on Adsorption of Phenol (at 25 mg/L initial concentration)

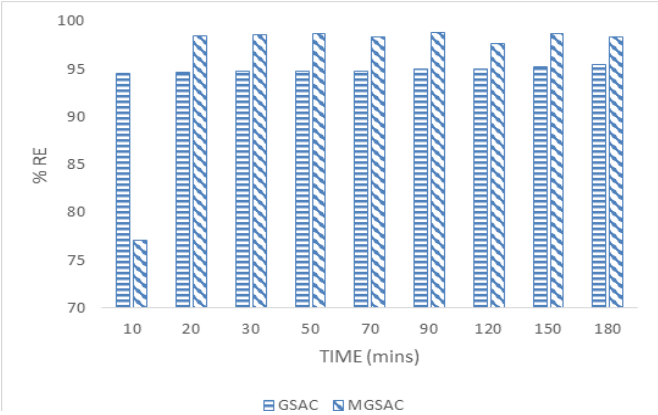

Figure 7. Effect of Contact Time on Percentage Removal of Pb(II) (at 25 mg/L initial concentration)

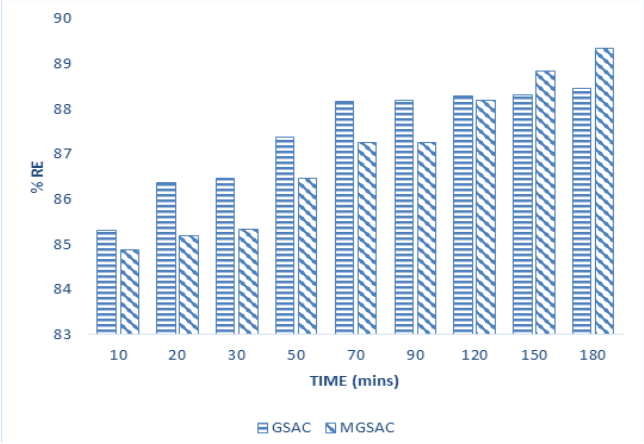

Figure 8. Effect of Time on Percentage Removal of Phenol (at 25 mg/L initial concentration)

The rapid uptake at the commencement of adsorption is due to a very high mass transfer driving force which reduces as the concentration of the pollutants in the solutions drops. The drop in 2% removal for MGSAC from 90 minutes to 120 minutes and then increase at 150 minutes was observed in Figure 7. This was only a slight drop and could be due to experimental error.

3.5.2 Effect of Adsorbent Dosage

The adsorption dosage varied from 0.2-1.0 g and the effect of each on adsorption capacity and removal efficiencies of Pb(II) and phenol are shown in Figures 9-12. These were conducted at 25 mg/L initial concentration, 25˚C, 200 rpm shaking speed and 180 minutes contact time. It was observed that the adsorption capacity for both GSAC and MGSAC had increased from 14.92 to 73.59 mg/g and 14.98 to 74.64 mg/g respectively. The removal efficiencies for both GSAC and MGSAC had increased from 94.46 to 98.12% and 99.52 to 99.92%, respectively.

As the adsorbent doses increase, the adsorption capacity and removal efficiency of Pb(II) and phenol

increase. This can be directly linked to the availability of adsorption sites with an increasing amount of adsorbent (Simha et al., 2016). It was also discovered that the adsorption capacity and removal efficiency of the MGSAC dosage were higher compared to the GSAC. Hence the modification improved the performance of the adsorbent.

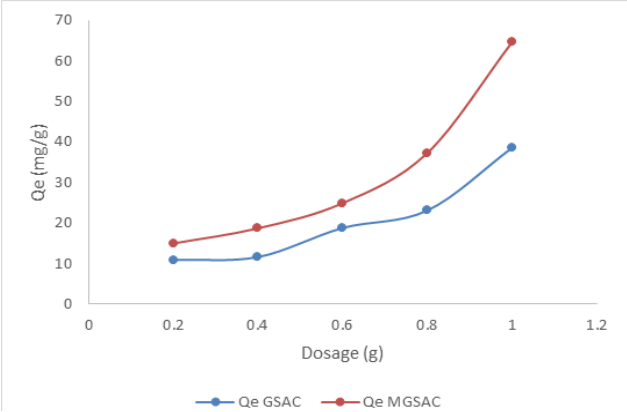

Figure 9. Effect of Dosage on Adsorption Capacity of Pb(II)

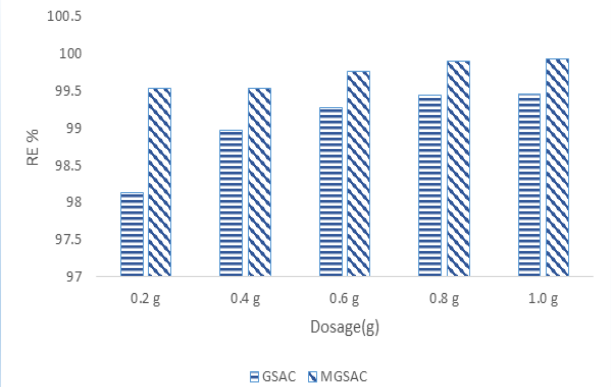

Figure 10. Effect of Dosage on Removal Efficiency of Pb(II)

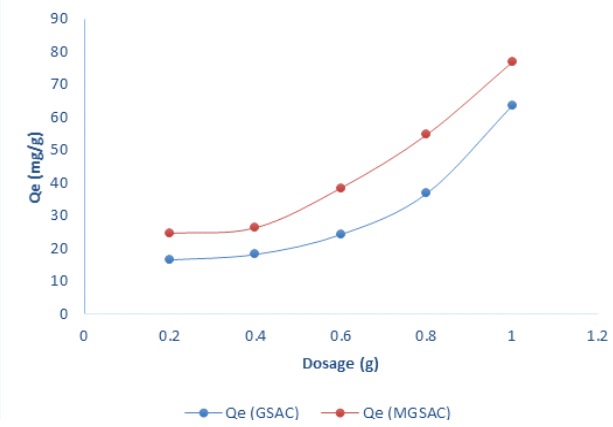

Figure 11. Effect of Dosage on Adsorption Capacity of Phenol

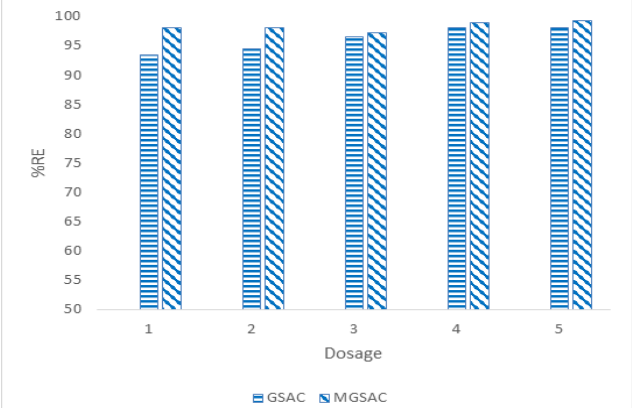

Figure 12. Effect of Dosage on Removal Efficiency of Phenol

3.5.3 Effect of Temperature

The effect of temperature and the impact was studied by varying temperature (35˚C, 45˚C, and 55˚C), The impact of the variation on adsorption capacity and removal efficiencies were investigated within the time interval of 15-55 min as shown in the Figure 13. These were conducted at 25 mg/L initial concentration, 200 rpm shaking speed and 0.2 g adsorbent in 100 ml aqueous solution. The MGSAC was observed to have a higher adsorption rate than the GSAC at the three temperatures. It was also observed that, as the temperature increased the adsorption capacity decreased, which means that the adsorption for Pb(II) and phenol with MGSAC are exothermic, and, a lower temperature is favourable for adsorption of phenol (Adeniyi and Ighalo, 2019). However, beyond the optimal threshold, there was no observable change in adsorption capacity with time (x-axis) due to the filled up pore spaces on the adsorbent.

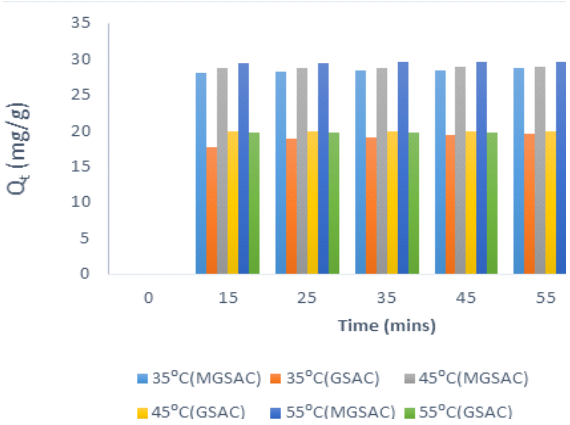

Figure 13. Plot of Qt against Time for Pb(II) at 35˚C, 45˚C, and 55˚C

3.6 Adsorption Equilibrium Isotherm

Three adsorption isotherm equations were used in the investigation of the adsorption experimental study: Langmuir, Freundlich and Temkin models. The

application of the three isotherm equations was compared by judging the correlation coefficient, R^2 between them. The Lanmuir plot of c_e/q_e versus q_e using the linearised equation was used. It was applied to determine the Langmuir parameters for the adsorption of Pb(II) and phenol unto both GSAC and MGSAC. The Langmuir constants were evaluated from the slope $1/q_m$ and intercept $1/(q_mK_L)$ as shown in Tables 5 and 6. The negative values of K_L and Q_L obtained from 25 mg/l to 125 mg/l concentrations for the GSAC indicated the inefficiency of Langmuir model to explain the adsorption process, likewise for the 25 mg/l to 125 mg/l in the MGSAC. But the parameters $1/q_m$ and $1/(q_mK_L)$ were positive from 25 mg/l – 125 mg/l for the GSAC, and 25 mg/l - 125 mg/l for the MGSAC.

Table 5. Isotherm Characteristics Parameters of Langmuir, Freundlich and Temkin Isotherm Constants for Pb(II) onto GSAC

	25 mg/l	50 mg/l	75 mg/l	100 mg/l	125 mg/l
Qexp (mg/g)	23.86	47.78	74.98	96.86	120.35
Langmuir					
Q_M (mg/g)	22.57	45.25	70.92	93.46	116.28
K_L (L/g)	15.82	8.5	141	8.91	5.375
R_L	0.02	0.02	9.5	0.001	0.001
R^2	1.00	1.00	1.00	1.00	1.00
Freundlich					
K_f (mg/g)	3.977	5.424	6.557	7.413	0.9994
n	1.3	1.6	1.8	2.0	2.1
R^2	0.93	0.95	0.94	0.94	0.95
Temkin					
β (mg^2/J^2)	166.2	43.98	281.1	1477	121.1
α (L/mg)	1.0	1.1	1.0	1.0	1.01
R^2	0.92	0.39	0.86	0.007	0.34

Table 6. Isotherm Characteristics Parameters of Langmuir, Freundlich and Temkin Isotherm Constants for Pb(II) onto MGSAC

	25 mg/l	50 mg/l	75 mg/l	100 mg/l	125 mg/l
Qexp (mg/g)	24.71	49.51	74.81	97.90	122.23
Langmuir					
Q_M (mg/g)	19.01	48.30	72.9	98.0	120.8
K_L (L/g)	1.14	6.9	137	113	2.0
R_L	0.03	0.002	9.7	8.0	0.003
R^2	0.99	1.00	1.00	0.99	0.99
Freundlich					
K_f (mg/g)	3.641	5.457	6.477	7.330	8.11
n	4.6	19.61	1.0	714.2	70.0
R^2	0.31	0.93	0.84	0.0071	0.32
Temkin					
β (mg^2/J^2)	166.2	85.3	21.15	62.45	43.66
α (L/mg)	1.0	1.0	1.59	1.0	1.1
R^2	0.95	0.94	0.93	0.65	0.94

The essential characteristics of Langmuir isotherm can be explained in terms of the separation factor (R_L). When $0 < R_L < 1$, the adsorption process is feasible. The values of R_L were less than 1 for both the GSAC and the MGSAC at the same concentrations (which means that they were favourable for the GSAC and MGSAC adsorption). The closeness of the value of the correlation coefficients (R^2) to 1 compared to the Freundlich and Temkin model indicated that Langmuir isotherm is the best-fit isotherm to describe the adsorption of Pb(II) and phenol unto GSAC and MGSAC.

The Freundlich plot of $\log q_e$ versus $\log C_e$ was used to determine the Freundlich isotherm parameters for the adsorption of Pb(II) and phenol unto both GSAC and MGSAC. The Freundlich parameters (n and K_F) and the correlation coefficients (R^2) are shown in Table 5 and 6. The Freundlich exponent, n, for the adsorption of Pb(II) indicated the favorability of the adsorption process. Generally, values of n in the range 2 – 10 represent good, 1 – 2 moderately good, and less than 1 poor adsorption characteristics (Babatunde et al., 2019). It was discovered that the R^2 of the MGSAC are higher than the GSAC, indicating higher adsorption capacity for Pb(II) molecules compared to GSAC.

The Temkin plot of q_e against $\ln C_e$ was used to determine the Temkin isotherm parameter for the adsorption of Pb(II) and phenol onto the adsorbent. The linear isotherm constants and coefficients of determination for both the GSAC and the MGSAC are presented in Table 5 and 6. It shows that the equilibrium binding constant (α) (L/mg) which corresponds to the maximum binding energy increased with increase in concentration (Olajire et al., 2016). The constant β which is related to the heat of adsorption equally increased with increase in concentration, but the heat of adsorption of all the molecules in the layer decreased linearly with coverage. The results implied that the affinity of the binding sites for lead and phenol increased with increase in concentration. The correlation coefficient (R^2) of the GSAC was higher compared to the MGSAC. However, the low correlation coefficient (R^2) of the Temkin model compared to the Freundlich suggested that this model was not more suitable to fit the adsorption of Pb(II) unto activated carbon produced from groundnut shell.

3.7 Kinetics Studies

The kinetic data were analysed using both the pseudo-first order and pseudo-second order equations. The pseudo-first order plot of log (q_e - q_t) versus time gave straight lines with values of K_1 and q_{cal}, calculated from the slopes ($-k_1$) and intercepts ($\ln q_e$) of the plots respectively. The calculated parameters were presented in Table 7.

The plot of the concentration 25-125 mg/L showed high correlation coefficients for both the GSAC and MGSAC. For the GSAC, the plot of 75 mg/L initial concentration has the highest correlation coefficient of 0.87 while the 100 mg/L has the lowest R^2 0.84. However, the MGSAC has the highest R^2 of 0.99 at 50 mg/L and the lowest of 0.91.

The values of k and q_e for the pseudo-second order model were calculated from the intercepts ($1/K_{e2}$) and slope ($1/q_e$) of the plots of t/q_t vs. t, and are presented in

Table 8. The closeness of the correlation coefficients (R^2) highest values to 1 for both GSAC and MGSAC indicated that the pseudo-second order was fit to describe kinetic data suggesting that, pore diffusion was the rate-limiting step. It can be deduced, that it was best-fit for the MGSAC compare to GSAC.

Table 7. Kinetic Parameters and Correlation Coefficients (R^2) Obtained for the First Order Models

Initial Conc. mg/l	GSAC			MGSAC		
	q_e (mg/g)	K_1 (min^{-1})	R^2	q_e (mg/g)	K_1 (min^{-1})	R^2
25	4.038	0.009	0.84	3.73	0.014	0.91
50	1.11	0.203	0.82	1.12	0.011	0.92
75	1.120	0.003	0.87	0.67	0.013	0.91
100	3.24	0.006	0.84	0.67	0.0053	0.93
125	2.438	0.015			0.022	0.94

Table 8. Kinetic Parameters and Correlation Coefficients (R^2) Obtained for the Second Order Models

Conc. mg/l	GSAC			MGSAC		
	q_e (mg/g)	K_2 (g/mg.min)	R^2	q_e (mg/g)	K_2 (g/mg.min)	R^2
25	23.80	0.158	0.99	24.70	0.18	1.00
50	47.78	0.07	0.99	49.00	0.04	1.00
75	71.78	0.19	0.99	74.80	0.02	1.00
100	96.86	0.02	0.81	99.0	0.30	1.00
125	120.34	0.08	0.99	122	1.33	1.00

3.8 Thermodynamic Studies

The standard enthalpy (ΔH°), standard free energy (ΔG°), and standard entropy (ΔS°) are considered to characterise the adsorption process due to the transfer of one mole of solute from the solution onto solid-liquid interface (Olajire et al. 2016). The parameters were determined by the plot of ln K_d against 1/T (Vant Hoff's plot). The partitioning coefficient K_d (L/mol) of the Pb(II) and phenol towards the activated carbon is an important parameter for examining the Pb(II) and phenol molecule migration through the MGSAC (see Table 9). The values of the ΔG° are negative except at 318 and 328 K at 15 min for the MGSAC. The values of ΔG° for the adsorption of Pb(II) on MGSAC was higher which indicated that adsorption process was spontaneous and feasible on the MGSAC except for the ones at temperature 318 K and 328 K respectively. The absolute decrease in a negative value of ΔG˚ as the temperature increased indicated that adsorption decreased with rising in temperature. This change in ΔG° value may be due to the increase in the degree of freedom which might enhance desorption rather than adsorption at high temperatures (Rani and Sud, 2015).

Generally, the range of free energy values (ΔG˚) for physio-sorption is between -20 and 0 KJ/mol while chemisorption is between -80 and -400 KJ/mol. The value of the ΔG° fell within the range of 0 to -20 kJ/mol for the adsorption process on MGSAC. The ΔH° values gotten were negative, which varied from -3.3250 kJ/mol to -21.3021 kJ/mol for MGSAC. This showed that the adsorption process of Pb(II) was exothermic (Babarinde and Onyiaocha 2016). It can be seen that the adsorption process on the MGSAC is tending towards chemisorption. The small negative values of ΔS° (-0.0210 to 0.0087 KJ/mol) MGSAC suggested the decreased randomness on solid/solute interface during the adsorption.

4. Conclusion

The groundnut shell activated carbon was produced by the impregnation of phosphoric acid in the right proportion and half of the prepared activated carbon was modified with $AgNO_3$ to improve the adsorptive property of the activated carbon. The FTIR was used for suggesting the surface chemistry of the GSAC and MGSAC indicated the large presence of O-H, C=O and N-H. There was the appearance of the -C≡C- after the modification of the activated carbon with $AgNO_3$. FTIR also show the functional molecules (Cellulose, hemicelluloses, lignin and pectin). SEM analysis revealed disordered pores over the carbon particle surface. The EDX analysis confirmed that carbon is the major element. The MGSAC has a higher adsorption capacity and percentage removal compared to the GSAC for all domains of factors.

Table 9. Thermodynamic Parameters for the Adsorption of Pb(II) onto MGSAC

Time (min)	Temperature (K)	K_d	ln K_d	ΔG (kJ/mol)	ΔH (KJ/mol)	ΔS (KJ/mol)
	308	2.5755	0.7246	-1.1239		
15	318	0.7286	-0.0831	0.1469	-20.6215	-0.567
	328	0.85	-0.1867	0.5678		
	308	2.5581	0.7119	-1.9578		
25	318	1.5035	0.1249	-0.9567	-12.3254	-0.751
	328	1.5493	0.1385	-0.5672		
	308	2.7408	1.7196	-3.4167		
35	318	1.669	0.4568	-1.47I7	-21.3021	-0.0944
	328	1.6298	1.3577	-0.8699		
	308	3.6314	2.3447	-8.4325		
45	318	1.8867	4.1695	-9.5794	-3.3250	-0.0087
	328	3.2692	2.6787	-3.7686		
	308	17.8333	2.8811	-7.3776		
55	318	11.5333	2.4615	-6.3948	-16.1248	-0.220
	328	13.6	2.4314	-7.6199		

The equilibrium data fitted best to the Langmuir isotherm model for the adsorption of Pb(II) on both the GSAC and MGSAC. The results also illustrated that the adsorption of Pb(II) onto both the GSAC and MGSAC fit best to the pseudo-second order.

The adsorption process was observed to be heterogeneous, exothermic and spontaneous. It can be deduced that groundnut shell is a good starting material in the production of activated carbon due to its high yield and good adsorption capacity. The modification of the activated carbon with silver nitrate is to increase the rate of adsorption, and to determine the performances of different adsorbate on the produced groundnut shell activated carbon for the investigations of the liquid phase and gaseous phase adsorption behaviours.

References:

Abussaud, B., Asmaly, H.A., Saleh, A., and Kumar, V. (2015), "Sorption of phenol from waters on activated carbon impregnated with iron oxide, aluminum oxide and titanium oxide", *Journal of Molecular Liquids*, Vol.213, pp.351-359 doi:http://dx.doi.org/10.1016/j.molliq.2015.08.044

Adeniyi, A.G., and Ighalo, J.O. (2019), "Biosorption of pollutants by plant leaves: An empirical review", *Journal of Environmental Chemical Engineering*, Vol.7, pp.103-100 doi:http://dx.doi.org/10.1016/j.jece.2019.103100

Adeniyi, A.G., Ighalo, J.O., and Onifade, D.V. (2020), "Biochar from the thermochemical conversion of orange (*Citrus sinensis*) peel and albedo: Product quality and potential applications", *Chemistry Africa*, Vol.3, pp.439-448 doi:http://dx.doi.org/10.1007/s42250-020-00119-6

Ali, A., Bilal, M., Khan, R., Farooq, R., and Siddique, M. (2018), "Ultrasound-assisted adsorption of phenol from aqueous solution by using spent black tea leaves", *Environmental Science and Pollution Research*, pp.1-11 doi:http://dx.doi.org/10.1007/s11356-018-2186-9

Amuda, O.S., Giwa, A.A., and Bello, I.A. (2007), "Removal of heavy metal from industrial wastewater using modified activated coconut shell carbon", *Biochemical Engineering Journal*, Vol.36, pp.174-181 doi:http://dx.doi.org/10.1016/j.bej.2007.02.013

Araujo, L.A., Bezerra, C.O., Cusioli, L.F., Silva, M.F., Nishi, L., Gomes, R.G., and Bergamasco, R. (2018), "Moringa oleifera biomass residue for the removal of pharmaceuticals from water", *Journal of Environmental Chemical Engineering*, Vol.6, pp.7192-7199

Babarinde, A., and Onyiaocha, G.O. (2016), "Equilibrium sorption of divalent metal ions onto groundnut (Arachis hypogaea) shell: Kinetics, isotherm and thermodynamics", Chem Int 2, Vol.2, No.1, pp. 27-46

Babatunde, E.O., Akolo, S.A., Ighalo, J.O., and Kovo, A.S. (2019), "Response surface optimisation of the adsorption of Cu (II) from aqueous solution by crab shell chitosan", Paper presented at *the 3rd International Engineering Conference*, Minna, Nigeria, September 24-26, pp.1-9

Canlas, J.J., Go, J.C., Mendoza, A.C., and Dimaano, M.N. (2019), "Talisay (*Terminalia catappa*) seed husk biochar for adsorption of lead (II) ions in artificially contaminated soil", In: MATEC Web of Conferences, 2019. EDP Sciences, p 04011

Eletta, O.A.A., Adeniyi, A.G., Ighalo, J.O., Onifade, D.V., and Ayandele, F.O. (2020), "Valorisation of cocoa (*Theobroma cacao*) pod husk as precursors for the production of absorbents for water treatment", *Environmental Technology Reviews*, Vol.9, pp.20-36 doi:http://dx.doi.org/10.1080/21622515.2020.1730983

Eletta, O.A.A., Ayandele, F.O., Adeniyi, A.G., and Ighalo, J.O. (2019), "Valorisation of sunflower (*Tithonia Diversifolia*) stalk for the removal of Pb(II) And Fe(II) from aqueous solutions", Proceedings of the 49th NSChE Annual Conference, Kaduna, Nigeria, November 13-16, pp 107-116

Eletta, O.A.A., and Ighalo, J.O. (2019), "A review of fish scales as a source of biosorbent for the removal of pollutants from industrial effluents", *Journal of Research Information in Civil Engineering*, Vol.16, pp.2479-2510 doi:http://dx.doi.org/10.13140/RG.2.2.20511.61604

Fadzil, F., Ibrahim, S., and Hanafiah M.A.K.M. (2016), "Adsorption of lead (II) onto organic acid modified rubber leaf powder: Batch and column studies", *Process Safety and Environmental Protection*, Vol.100, pp.1-8

Farag, I.A.A., and Zahran, A.A. (2014), "Groundnut (*Arachis hypogaea L*) growth and yield responses to seed irradiation and mineral fertilisation", *IOSR Journal of Agriculture and Veterinary Science*, Vol.7, pp.63-70

Fauzia, S., Aziz, H., Dahlan, D., and Zein, R. (2017), "Study of equilibrium, kinetic and thermodynamic for removal of Pb(II) in aqueous solution using Sago bark (*Metroxylon sago*)", *Proceedings of the 3rd International Symposium on Current Progress in Mathematics and Sciences (ISCPMS2017)*, Bali, Indonesia, July 26-27, pp.1-8. doi:http://dx.doi.org/10.1063/1.5064078

Gupta, A., and Rafe, M.A. (2013), Removal of phenol from wastewater using mango peel", *International Journal of Engineering and Technology Research*, Vol.1, pp.58-62

Ighalo, J.O., and Adeniyi, A,G. (2020a), "Adsorption of pollutants by plant bark derived adsorbents: An empirical review", *Journal of Water Process Engineering*, Vol.35, pp.101228 doi:http://dx.doi.org/10.1016/j.jwpe.2020.101228

Ighalo, J.O., and Adeniyi, A.G. (2020b), "A mini-review of the morphological poperties of biosorbents derived from plant leaves", *SN Applied Sciences*, Vol.2, pp.509 doi:http://dx.doi.org/10.1007/s42452-020-2335-x

Ighalo, J.O., and Adeniyi, A.G. (2020c), "Mitigation of Diclofenac Pollution in Aqueous Media by Adsorption", *ChemBioEng Reviews*, Vol.7, pp,50-64 doi:http://dx.doi.org/10.1002/cben.201900020

Ighalo, J.O., and Adeniyi, A.G. (2020d), "Statistical modelling and optimisation of the biosorption of Cd(II) and Pb(II) onto dead biomass of pseudomonas aeruginosa", *Chemical Product and Process Modelling*, pp.1-10. doi:http://dx.doi.org/10.1515/cppm-2019-0139

Ighalo, J.O., Adeniyi, A.G., Eletta, O.A.A., and Arowoyele, L.T. (2020a), "Competitive adsorption of Pb(II), Cu(II), Fe(II) and Zn(II) from aqueous media using biochar from oil Palm (*Elaeis guineensis*) fibers: A kinetic and equilibrium study", *Indian Chemical Engineer*, pp.1-11 doi:http://dx.doi.org/10.1080/00194506.2020.1787870

Ighalo, J.O., and Eletta, A.A.O. (2020), "Recent advances in the biosorption of pollutants by fish scales: A mini-review", *Chemical Engineering Communications*, p.1-12 doi:http://dx.doi.org/10.1080/00986445.2020.1771322

Ighalo, J.O., Tijani, I.O., Ajala, J.O., Ayandele, F.O., Eletta, O.A.A., and Adeniyi, A.G. (2020b), "Competitive biosorption of Pb(II) and Cu(II) by functionalised micropogonias undulates scales", *Recent Innovations in Chemical Engineering*, Vol.13 doi:http://dx.doi.org/10.2174/2405520413999200623174612

Karimpour, M., Ashrafi, S.D., Taghavi, K., Mojtahedi, A., Roohbakhsh, E., and Naghipour, D. (2018), "Adsorption of cadmium and lead onto live and dead cell mass of pseudomonas aeruginosa: A dataset", *Data in Brief*, Vol.18, pp.1185-1192

Lütke, S.F., Igansi, A.V., Pegoraro, L., Dotto, G.L., Pinto, L.A., and Cadaval, Jr.T.R. (2019), "Preparation of activated carbon from black wattle bark waste and its application for phenol adsorption", *Journal of Environmental Chemical Engineering*, Vol.7, No.5, DOI: https://doi.org/10.1016/j.jece.2019.103396

Mall, I.D., Srivastava, V.C., and Agarwal, N.K. (2006), "Removal of orange-G and methyl violet dyes by adsorption onto bagasse fly ash—kinetic study and equilibrium isotherm analyses", *Dyes and Pigments*, Vol.69, pp.210-223

Moelyaningrum, A.D. (2018), "The potential of cacao pod rind waste (*Theobroma cacao*) to adsorb heavy metal (Pb and Cd) in water", In: *Sustainable Future for Human Security*. Springer, pp 265-276

Olajire, A.A., Abidemi, J.J., Lateef, A., and Benson, N.U. (2016), "Adsorptive desulphuirisation of model oil by Ag nanoparticles-modified activated carbon prepared from brewer's spent grains", *Biochemical Pharmacology*, doi:http://dx.doi.org/10.1016/j.jece.2016.11.033

Olarinmoye, O., Bakare, A., Ugwumba, O., and Hein, A. (2016), "Quantification of pharmaceutical residues in wastewater impacted surface waters and sewage sludge from Lagos, Nigeria", *Journal of Environmental Chemistry and Ecotoxicology*, Vol.8, pp.14-24

Rai, P., Gautam, R.K., Banerjee, S., Rawat, V., and Chattopadhyaya, M. (2015), "Synthesis and characterisation of a novel $SnFe_2O_4$ activated carbon magnetic nanocomposite and its effectiveness in the removal of crystal violet from aqueous solution", *Journal of Environmental Chemical Engineering*, Vol. 3, pp.2281-2291

Rani, S., and Sud, D. (2015), "Effect of temperature on adsorption-desorption behaviour of triazophos in Indian soils", *Plant, Soil and Environment*, Vol.61, pp.36-42

Rashid, R.A., Jawad, A.H., Ishak, M.A.M., and Kasim, N.N. (2016), KOH-activated carbon developed from biomass waste: adsorption equilibrium, kinetic and thermodynamic studies for methylene blue uptake", *Desalination and Water Treatment*, Vol.57, pp.27226-27236

Sarkar, M., Acharya, P.K., and Bhattacharya, B. (2003), "Modelling the adsorption kinetics of some priority organic pollutants in water from diffusion and activation energy parameters", *Journal of Colloid and Interface Science*, Vol.266, pp.28-32 doi:http://dx.doi.org/10.1016/S0021-9797(03)00551-4

Simha, P., Yadav, A., Pinjari, D., and Pandit, A.B. (2016), "On the behaviour, mechanistic modelling and interaction of biochar and crop fertilisers in aqueous solutions", *Resource-Efficient Technologies*, Vol.2, pp.133-142

Snyder, S., Lue-Hing, C., Cotruvo, J., and Jörg, E.D., Eaton, A., Richard, C.P., and Schlenk, D. (2010), *Pharmaceuticals in the Water Environment*, National Association of Clean Water Agencies (NACWA)

Sonawane, B.K., and Korake, S.R. (2016), "Review on removal of phenol from wastewater using low cost adsorbent", *International Journal of Science, Engineering and Technology Research*, Vol.5, pp.2249-2253

Trubetskaya, A., Kling, J., Ershag, O., Attard, T.M., and Schröder, E. (2019), "Removal of phenol and chlorine from wastewater using steam activated biomass soot and tire carbon black", *Journal of Hazardous Materials,* Vol.365, pp.846-856

Wang, L., Zhang, J., Zhao, R., Li, Y., Li, C., and Zhang, C. (2010), "Adsorption of Pb (II) on activated carbon prepared from Polygonum orientale Linn: Kinetics, isotherms, pH, and ionic strength studies", *Bioresource Technology*, Vol.101, pp.5808-5814 doi:http://dx.doi.org/10.1016/j.biortech.2010.02.099

Yakout, S., and El-Deen, G.S. (2016), "Characterisation of activated carbon prepared by phosphoric acid activation of olive stones", *Arabian Journal of Chemistry,* Vol.9, pp.1155-1162

Yang, G., Tang, L., Zeng, G., Cai, Y., Tang, J., Pang, Y., and Zhou, Y. (2015), "Simultaneous removal of lead and phenol contamination from water by nitrogen-functionalised magnetic ordered mesoporous carbon", *Chemical Engineering Journal*, Vol.259, pp.854-864 doi:http://dx.doi.org/10.1016/j.cej.2014.08.081.

Authors' Biographical Notes:

Omodele A. A. Eletta *is an associate professor at the Department of Chemical Engineering University of Ilorin. She obtained her Bachelor Degree in Chemical Engineering (1986) from the University of Lagos, Nigeria. She also obtained her Masters' Degree in Chemical Engineering (1996) from the University of Lagos, Nigeria. She had her PhD in Chemistry (Environmental/Analytical Chemistry) (2005) from the University of Ilorin, Nigeria. Her research interests include environmental engineering with a special focus on the remediation of water pollution by adsorption.*

Ibrahim O. Tijani *obtained a Bachelor Degree in Chemical Engineering (2015) from Ladoke Akintola University of Technology, Ogbomoso, Nigeria. He also obtained a Masters' Degree in Chemical Engineering (2020) from the University of Ilorin, Nigeria. His research interest includes environmental pollution control with a special focus on the adsorption process.*

Joshua O. Ighalo *obtained a Bachelor Degree in Chemical Engineering (2015) from the University of Benin, Nigeria. He also obtained a Masters' Degree in Chemical Engineering (2020) from the University of Ilorin, Nigeria. His research interest includes computer-aided modelling and optimisation of chemical process systems, biofuels, solid waste management and environmental pollution control.*

■